



# Impact of temperature on LVI-damage and tensile and compressive residual strength of CFRP

Johann Körbelin\*, Chiara Dreiner, Bodo Fiedler

Hamburg University of Technology, Institute of Polymer and Composites, Denickestraße 15, Hamburg D-21073, Germany

## ARTICLE INFO

### Keywords:

Impact behaviour  
Damage Tolerance  
Delamination  
Thermomechanical  
Fracture

## ABSTRACT

This study investigates the influence of temperature and impact-energy on low-velocity impact damage in CFRP and the resulting residual tensile and compressive strength. Impacts were introduced at  $-20^{\circ}\text{C}$ ,  $20^{\circ}\text{C}$  and  $80^{\circ}\text{C}$ , which are moderate temperature compared to the glass transition temperature of  $203^{\circ}\text{C}$  of the used CFRP. A change in temperature leads to a substantial change in damage behaviour. With increasing temperature, the delamination area is reduced, and at  $80^{\circ}\text{C}$  fibre-failure occurs on the impacted side. The residual tensile strength was tested at  $20^{\circ}\text{C}$  utilising a new jig, which counteracts the stresses resulting from free-edge effects and thus prevents that edge delaminations are overshadowing the effect of the impact damage due to the specimen size. The fibre failure reduces the residual tensile strength significantly compared to the damage resulting from impactation at  $20^{\circ}\text{C}$ . The compressive residual strength was determined at  $20^{\circ}\text{C}$  and  $80^{\circ}\text{C}$ . The results point out that the temperature mainly determines the residual compressive strength. Consequently, it is essential to identify the material's behaviour in the range of the in-service temperatures, even if they are far away from the glass transition temperature, to evaluate the damage tolerance and performance.

## 1. Introduction

Carbon fibre reinforced plastics (CFRP) are used in high-performance applications where excellent density-specific stiffness and strength are needed. Their brittle behaviour, combined with a layered structure results in a low out of plane strength. As a result, impact damage resistance is a significant concern with CFRP structures. Of particular interest are low-velocity impact (LVI) damages, which often result in barely visible impact damage (BVID). These damages are difficult to detect during operation and result in a significant reduction in strength [1]. Following the concept of “damage tolerance” structures must be designed that the planned load capability can be maintained with BVID, as the presence of BVID must be assumed [2–4].

As a result, a comprehensive understanding of the damage caused by LVI and the resulting residual strength is essential in order to design safe, lightweight and damage-tolerant structures. Consequently, LVI-damage and the resulting residual strength has been a research focus for decades [1,5]. Nevertheless, there are still open questions, especially concerning the impact of environmental factors. Composite structures experience different climates and therefore various temperatures during operation [6]. The temperature influences the elastic and damage behaviour of CFRP [7–11]. Consequently, a straightforward an-

swer on how temperature is influencing the damage process cannot be given since different effects like matrix softening, stress relaxation and the reduction of thermal stresses combine to influence the failure process.

This work continues a study by Körbelin et al. [12] in which the influence of different impact energies and elevated ambient temperatures on LVI damage was investigated. Impactation was performed at temperatures between  $20^{\circ}\text{C}$  and  $80^{\circ}\text{C}$ , and therefore below the materials glass transition temperature ( $T_g$ ) of  $203^{\circ}\text{C}$ . It was found that even small changes in temperature are influencing the damage behaviour significantly. Projected delamination size is decreasing with increasing temperature, which was also found by several studies [13,14]. However, severe fibre failure on the impacted side occurs at elevated temperatures. The residual compressive strength at  $20^{\circ}\text{C}$  nonetheless is mainly dependent on the delamination size and therefore increasing with impactation temperature [15]. But temperature is adding more complexity to damage assessment, as damage resulting from significantly different impact energies can have the same effect on the residual compressive strength when impacted at different temperatures. Due to occurring fibre damage and increasing indentation depth with temperature, the visual damage severity does not correlate with the residual compressive strength. From these results two questions follow:

\* Corresponding author.

E-mail address: [johann.koerbelin@tuhh.de](mailto:johann.koerbelin@tuhh.de) (J. Körbelin).

- How is the residual strength influenced by elevated temperature, if already a small change in temperature is causing a significant change in impact damage behaviour?
- Does fibre failure occurring at an elevated temperature significantly affect the residual tensile strength?

To answer these questions, this study tries to examine the most critical parameter combination in reference to the residual strength after impact.

Studies investigating the influence of temperature on LVI-damage are sparse. Gómez-del Río et al. [16] performed impacts at low temperatures ranging from 20 °C to −150 °C and found that cooling the laminate during impact has a similar effect as increasing the impact energy. The more extensive damage at lower temperatures is a result of lower specific fracture energy of the epoxy matrix combined with increasing inter-laminar thermal stresses. With decreasing temperature larger matrix cracking, delamination extension and deeper indentation on the impact side and more severe fibre-matrix debonding and fibre fracture on the opposite face was observed [16]. This larger delamination area could lead to a lower residual compressive strength, as residual strength of cross-ply or quasi-isotropic laminates in compression loading after impact is mainly dependent on delamination size and distribution in thickness direction inside the laminate [15]. However, the effect of a larger delamination size caused by low ambient temperature could be opposed at lower temperatures by a change in the mechanical properties, as the mechanical properties of the epoxy matrix depend largely on the operation temperature correlated with the glass transition temperature  $T_g$  [17]. Nearly all mechanical properties of the composite are changing with temperature, even well below  $T_g$ . The compressive modulus, strength and failure strain are decreasing with increasing temperature [10]. The shear strength and modulus also decrease, and the failure strain increases [10]. Still, studies which deal with the effect of temperature on the residual strength are sparse. Saez et al. [18] investigated the residual compressive strength of CFRP-laminates at 20 °C, −60 °C and −150 °C, and found that for quasi-isotropic laminates the compressive strength is not changing significantly when lowering the temperature. The residual compressive strength retention factor is ranging from 30 to 36 %. However, only thin samples were tested 1.6 mm which probably has to lead to a low extent to delamination damage, which could lead to a low sensitivity to ambient temperature. To the author's knowledge, no studies on the influence on elevated temperature on the compressive residual strength of CFRP have been published. From literature review the most critical parameter set could be the impactation at low temperature, leading to extensive delamination damage and afterwards compressive loading at elevated temperature. Nettles [11] investigated the influence of temperature on the open hole compressive (OHC) strength and found that the strength and fracture strain are decreasing with rising temperature. However, the damage resulting from impact damage could be more sensitive to temperature in residual strength testing because, due to the delamination damage, it is mainly stability driven [5,19].

The influence of impact damage on the residual tensile strength has also been of considerable research [1,5,19]. Generally, the residual strength is significantly reduced, which is accounted to stress concentrations resulting from impact damage [5]. But studies that attribute individual failure modes to the change in residual strength are scarce. Zhou et al. [20] investigated the influence of different layouts, impactor diameters, impact angle and energy on the residual strength. They found that fibre damage is occurring for their parameter set on the top side of the specimen around the contact area with the impactor, regardless of impactor size. The severity of fibre failure is increasing with decreasing impactor diameter, which is also reducing the residual tensile strength. However, the delaminations are spanning the whole width of the sample for nearly all parameter sets. Therefore the sensitivity of the strength to different occurring damage modes could be reduced, which highlights that testing of small specimens and evaluating the residual strength is generally a challenge [21]. Often during LVI-testing no fibre failure oc-

curs on either side of the specimen, as this usually occurs at higher impact energy [1]. As a result the change from no fibre failure to extensive fibre failure on the impacted side could influence the residual strength considerably.

## 2. Materials and experimental procedure

### 2.1. Material

Specimens were manufactured from Hexcel Hexply M21/35 %/268/T800S prepreg [22]. The layout was a quasi-isotropic layout  $[45/0/-45/90]_{2S}$  with a resulting thickness of 4.08 mm, chosen according to ASTM D7136 M [23]. The samples were cured in an autoclave, according to the manufacturer's specification. According to the specification, this results in a glass transition temperature of 203 °C. Every manufactured plate was inspected via ultrasonic C-scans for manufacturing flaws. The dimensions of the compressive specimen were chosen according to ASTM D7137 M, see Fig. 1 [24].

For determining the residual tensile strength, this specimen size of the compressive specimen was not practical, as no available machine could apply the tensile force required to fracture the sample. Therefore the width of the specimen was scaled so that the undamaged strength could be tested with available 250 kN grips. This resulted in a specimen width of 60 mm and a length of 250 mm, in order to apply the machine grips. The resulting specimen size is shown in Fig. 2.

The specimens were cut on a diamond blade saw, the edges were polished up to 2000 grit. The dimensional tolerances of all specimens were within the tolerance specified in ASTM D7136 M [23]. Prior testing all specimen were dried for 24h in a vacuum oven at 40 °C and then stored in a controlled climate for seven days at 23 °C with 50 % relative humidity. In addition, specimens for determining the compressive strength were made from the same test plates. The specimens were tabbed and cut according to ASTM D6641 M [25].

### 2.2. Impaction

The impact damage was introduced using a drop tower. For impaction of the compressive specimen, an uninstrumented droptower from CEAST with an anti-rebound device was used. The clamping was according to ASTM D7136 M [23], see Fig. 1. The boundary condition of this fixture is essentially simply supported. The impactor nose had a semi-spherical tip with a diameter of 20 mm. The mass and drop height was varied to keep the impact velocity approximately constant for different impact energies, see table 1. Four specimen for each parameter set were impacted.

For the impaction of the tensile specimens, due to the different clamping setup, a Primus 1700 Plus from Coesfeld Materialtest drop tower was used. It was also equipped with an anti-rebound device and utilized a semi-spherical tip with a diameter of 12.5 mm and uninstrumented. The clamping was essentially a 40 % scaled-down version of the clamping proposed in ASTM 7136 M [24], in order to achieve a similar loading setup with the smaller width samples. Impact-energy was chosen, supported by a preliminary test campaign so that the delamination growth does not reach the edge of the specimens, as this would influence the damage sequence as well as the occurring damage modes during impaction. Additionally, during residual tensile strength determination, the load distribution and progressive damage sequence would not be realistic, because load diversion in the laminate would be prevented due to extensive delamination. The impact parameters are combined in Table 2. Five specimen for each parameter set were impacted

Before impaction samples were tempered in a Memmert CTC256 climate chamber and then impacted within 10 s after removal, while the temperature was continuously monitored with thermocouples. Temperatures were chosen similar to [12]. For the compressive specimens, the main objective was to evaluate the influence of increased ambient temperature on the residual strength and determine possible critical loading

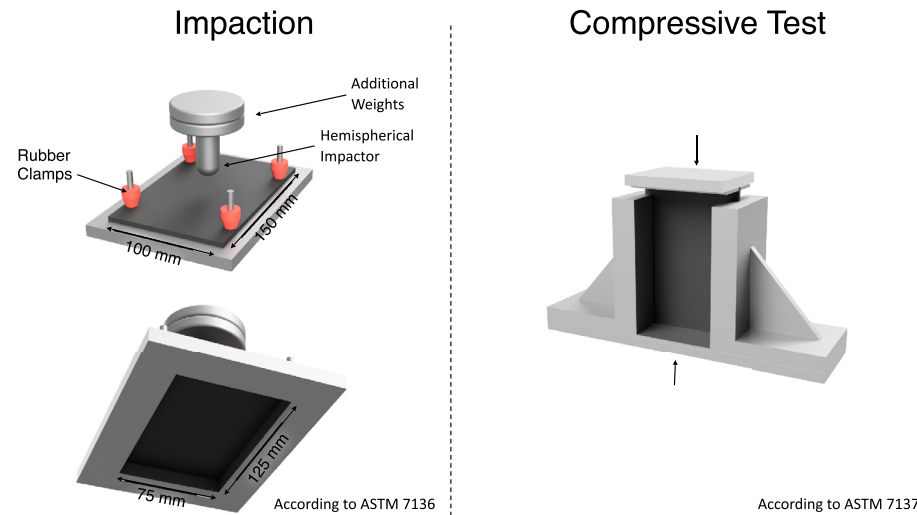


**Fig. 1.** Setup for the impactation of the compressive specimen (left) and the determination of the compressive residual strength (right).

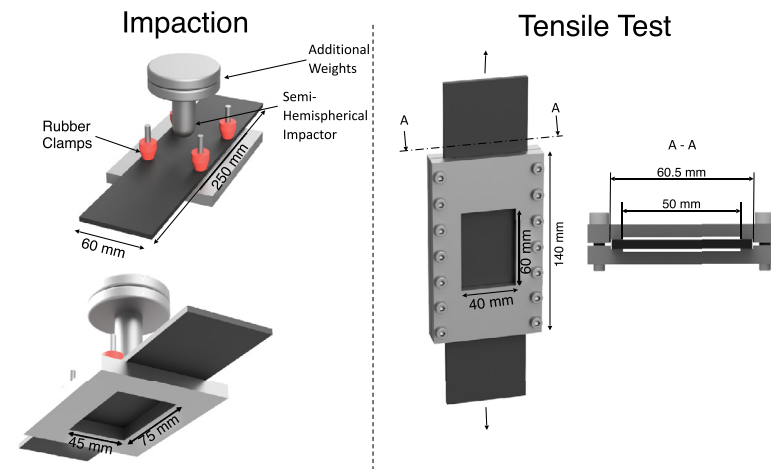


**Fig. 2.** Setup for the impactation of the tensile specimens (left) and the tensile residual strength test setup showing the edge-delamination suppression clamping (right).

**Table 1**  
Impactation parameters for compressive specimens.

Impact Energy [J]	Impactor Mass [kg]	Drop Height [mm]	Impact Velocity [ $\frac{m}{s}$ ]	Impactor Diameter [mm]
15	4.45	340	2.60	20
21	5.47	390	2.77	20

**Table 2**  
Impactation parameters for tensile specimens.

Impact Energy [J]	Impactor Mass [kg]	Drop Height [mm]	Impact Velocity [ $\frac{m}{s}$ ]	Impactor Diameter [mm]
25	5.34	477	3.06	12

scenarios. Therefore impacts were performed at  $-20^{\circ}\text{C}$  and  $80^{\circ}\text{C}$  and additionally for comparison at  $20^{\circ}\text{C}$ . The residual tensile strength was determined to evaluate the influence of the occurring fibre failure at elevated temperature. Therefore the impactation took place at  $80^{\circ}\text{C}$  and additionally for comparison at  $20^{\circ}\text{C}$ .

### 2.3. Damage characterization

After impactation, different non-destructive and destructive test methods were used to assess the damage in the samples and later evaluate the influence on the residual strength.

Ultrasonic C-scans were carried out with a USPC 3040 DAC from Ingenieurbüro Dr. Hillger. The system has a resolution of 20MHz and an amplification of up to 106dB in 0.5dB steps. Testing was performed with water as a coupling medium between the sample and an STS 6MHz probe from Karl Deutsch GmbH. The ultrasound speed in the specimen was calibrated by measuring the sample thickness and adjusting the velocity until the measured thicknesses matched. With the back wall echo, the projected delamination area was determined. The image was converted into a binary picture using a threshold, which was kept constant for all scans. The area was then determined by inverting the binary picture and summing up the area of all black pixels.

The permanent deformation of the samples on the impacted side was examined by scanning the surface with optical confocal microscopy using an Alicona G4 microscope. The resolution in the vertical direction was hereby  $0.41\mu\text{m}$ . The permanent deformation was measured with randomised specimen order within a week after impactation. Micrographs were taken for every impact temperature and impact energy of the compressive specimens. The specimens were cut through the middle, along the short side of the specimen and subsequently polished up to  $1\mu\text{m}$  using a diamond polishing suspension. The microscope pictures were taken with a Keyence VHX 6500 with 100x magnification.

## 2.4. Residual strength testing

The compressive strength and residual compressive strength tests were performed at  $20^\circ\text{C}$  and  $80^\circ\text{C}$  with a Zwick Z400 universal testing machine equipped with a temperature chamber. For residual strength testing a fixture according to ASTM 7137 M [24] was utilised, see Fig. 1. Five specimen per parameter set were tested. The residual strength was calculated from the force-displacement data using:

$$\sigma_c = \frac{|F_{min}|}{b \cdot t} \quad (1)$$

where  $\sigma_c$  is the residual compressive strength,  $|F_{min}|$  absolute value max. force in the compression test,  $b$  the width of the specimen and  $t$  the thickness. For the undamaged specimen, a hydraulic clamping fixture, according to ASTM D 6641 M [25], was utilised.

## 2.5. Tensile testing

Quasi-Isotropic laminates always exhibit edge stresses at the free edges, due to orthotropic ply behaviour, which lead to free edge stresses, which induce delamination [26]. In quasi-isotropic laminates on coupon level, this damage mechanism is one of the dominant mechanisms of damage. However, this does not correspond to laminated panels where stress concentrations as a result of impact damage occur at a greater distance from the edge. In this case, the stress concentration and edge delamination would not influence each other significantly. To achieve this behaviour also at the coupon level, a clamping device, which counteracts the peel stresses at the free edges of the specimens and thus suppresses edge delamination growth is used. The clamping is shown in Fig. 2. The edges of the sample are clamped on a width of 5 mm on each side. In order to decrease friction between the clamping and the specimen, PTFE-tape was applied on the clamping. As a result, the influence of the impact damage on the residual strength is not masked by the edge delamination damage. A window with a width of 40 mm and a height of 60 mm in the middle of the clamping device enables the usage of digital image correlation during testing. A change in tensile-strain-distribution as a result of the clamping could not be observed.

The residual tensile strength tests were carried out at  $20^\circ\text{C}$  with an Instron 8802 servo-hydraulic test system equipped with hydraulic grips and a 250 kN force transducer. Additionally, a digital image correlation system Aramis G4 from GOM was used. The residual tensile strength was determined using the force-displacement data:

$$\sigma_t = \frac{F_{max}}{b \cdot t} \quad (2)$$

where  $\sigma_t$  is the residual tensile strength,  $F_{max}$  is the maximum force in the compression test,  $b$  the width of the specimen and  $t$  the thickness.

## 3. Results

### 3.1. Compression specimens

In Fig. 3, the projected delamination area of the tested specimen is shown. The projected delamination area increases with the impact energy and decreasing temperature. The projected delamination area depends strongly on the environmental e.g. the temperature is decreased

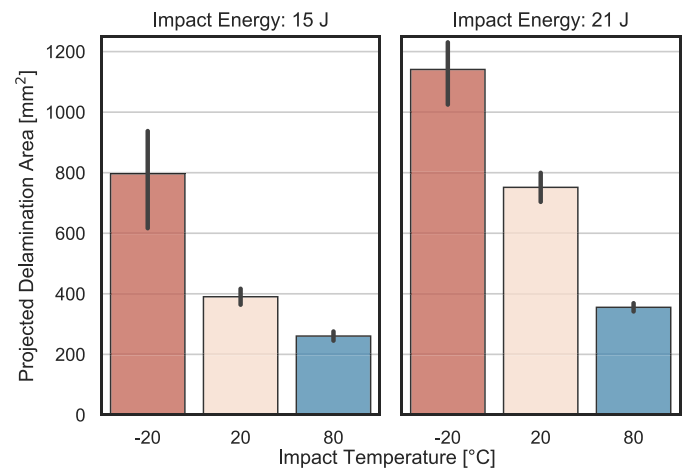


Fig. 3. Projected delamination area, determined from the ultrasonic C-scan.

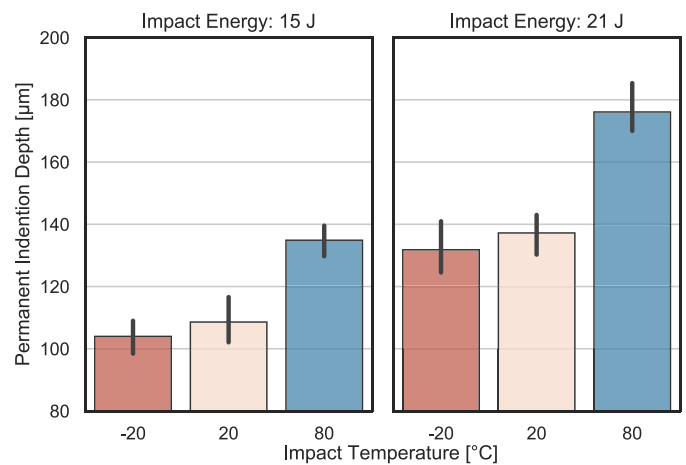
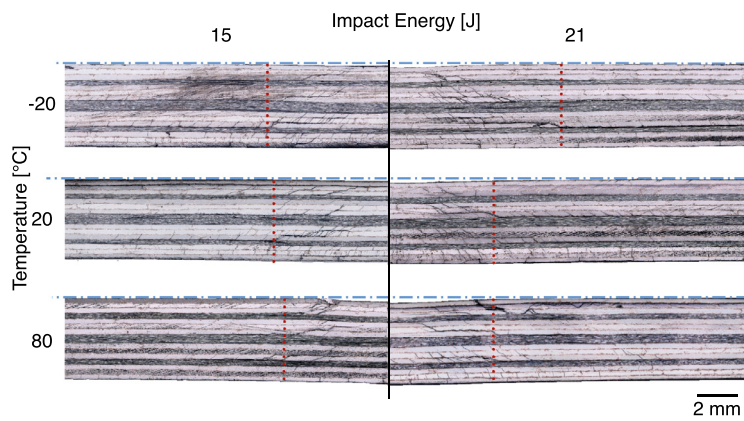


Fig. 4. Permanent indentation depth of the compressive specimens.

from  $20^\circ\text{C}$  to  $-20^\circ\text{C}$  at 15J impact energy, the projected delamination area is increased by 104.12 %. When taking temperature and impact energy into account it becomes apparent, that their relationship is not unique which means, that a certain projected delamination area cannot be associated with an impactation parameter set. The permanent indentation depth is shown in Fig. 4 and exhibits qualitatively an inverse relationship to the projected delamination area. The depth is increasing with impact energy and temperature. However, still the permanent indentation depths are well below visible impact damage limit of  $0.5\text{ mm}$  [27,28], energy and temperature are no longer unique. These effects can also be seen in the microsections, see Fig. 5.

Here the blue line is a straight reference line, which makes the increasing permanent indentation depth more evident. In general the microsection reveals, that the damage at  $-20^\circ\text{C}$  and  $20^\circ\text{C}$  exhibits the classic cone shape of the damage, whereas the matrix damage at  $80^\circ\text{C}$  is distributed more or less cylindrical. Which is also reflected in the permanent indentation, which is becoming more localised. The effect of compressive fibre failure on the matrix damage is visible at  $80^\circ\text{C}$  on the top side of the specimen, which was also shown by Körbelin et al. [12]. A change in delamination behaviour in dependence of the temperature is also visible, especially with 21J impact energy. The delamination at  $-20^\circ\text{C}$  is exhibiting larger delaminations with a more severe crack opening in the lowest  $45^\circ/90^\circ$  interface compared to the impacts at higher temperatures.



**Fig. 5.** Microsection through the short side of the impacted specimen at  $-20^{\circ}\text{C}$ ,  $20^{\circ}\text{C}$  and  $80^{\circ}\text{C}$ . The blue line is a reference to highlight the different impact depth. The red line is marking the begin of the permanent deformation.

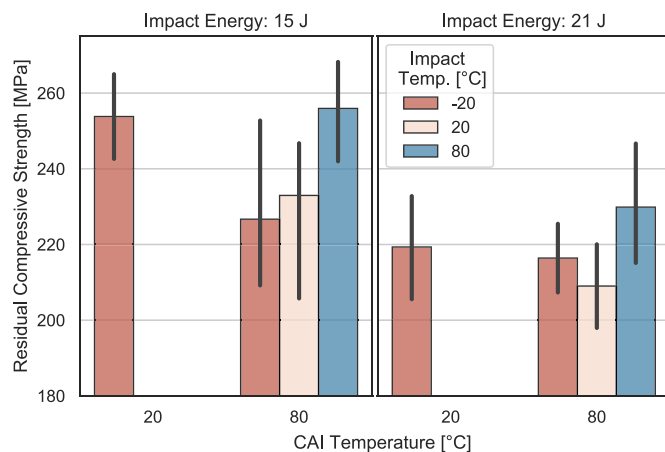


**Fig. 6.** Compressive residual strength after impactation at  $20^{\circ}\text{C}$  and  $80^{\circ}\text{C}$ .

In Fig. 6, the residual compressive strength of the tested parameters is shown. The residual strength of the 15J impacts is displaying a strong dependency to both, the impact temperature and the temperature during compressive testing. At  $-20^{\circ}\text{C}$  impact temperature the residual strength decreases by 10.6 %, if the temperature is increased from  $20^{\circ}\text{C}$  to  $80^{\circ}\text{C}$  for the compressive test. The residual strength of the impact at  $20^{\circ}\text{C}$  and  $80^{\circ}\text{C}$  is 8.3 % lower than the residual strength of the impact at  $-20^{\circ}\text{C}$  and residual strength at  $20^{\circ}\text{C}$ . Only the impact  $80^{\circ}\text{C}$  has a similar residual strength as the impact at  $-20^{\circ}\text{C}$  and residual strength at  $20^{\circ}\text{C}$ . The behaviour of specimens with 21J impact energy is different. The spread of data overall is much narrower. Consequently, the residual strength of samples impacted at  $-20^{\circ}\text{C}$  and  $20^{\circ}\text{C}$  is approximately the same, only at  $80^{\circ}\text{C}$  impactation the residual strength is slightly higher.

The undamaged compressive strength of the laminate is also strongly temperature-dependent. At  $20^{\circ}\text{C}$  the strength is 607 MPa with a mean error of 36.45 MPa. At  $80^{\circ}\text{C}$  the strength is reduced by 30.64 % to 421 MPa with a mean error of 16 MPa.

### 3.2. Tensile specimens

The indentation depths see Fig. 7, exhibits similar behaviour to the compressive specimens, which confirms that the altered clamping does not mark the temperature sensitivity of the damage development. When the temperature is increased to  $80^{\circ}\text{C}$  the indentation depth is growing by 36.31 %. The permanent indentation is also below visibility limit, for all impactation parameters tested. [27,28].

The delamination area is also exhibiting a similar behaviour to the compressive specimen, see Fig. 8, although the scatter is higher. This is due to the different fixtures used. The delamination damage is visualised

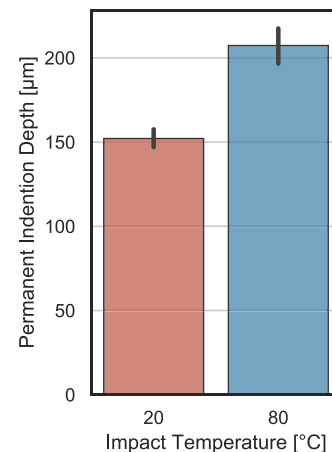


**Fig. 7.** Permanent indentation depth for 25J impacts on tensile specimen at  $20^{\circ}\text{C}$  and  $80^{\circ}\text{C}$ .

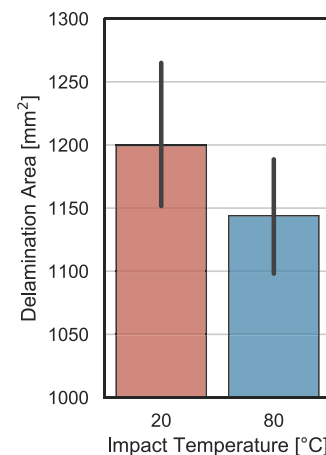


**Fig. 8.** Projected delamination area of tensile specimen for impacts with 25J at  $20^{\circ}\text{C}$  and  $80^{\circ}\text{C}$ .

in Fig. 9, displaying the defect echo of the C-scan in comparison to the sample and fixture size. It is visible that the delamination damage is developing almost over the whole width of the support frame distance. This is often the case for small fixtures [13,20], leading to a smaller sensitivity and a higher scatter. The delamination size reduced by 4.3 %.

Even though clamping has a significant influence on the damage resulting from LVI-Impact, a similar fibre failure pattern is developing on the impactation side of the specimens, see Körbelin et al. [12]. In Fig. 10,

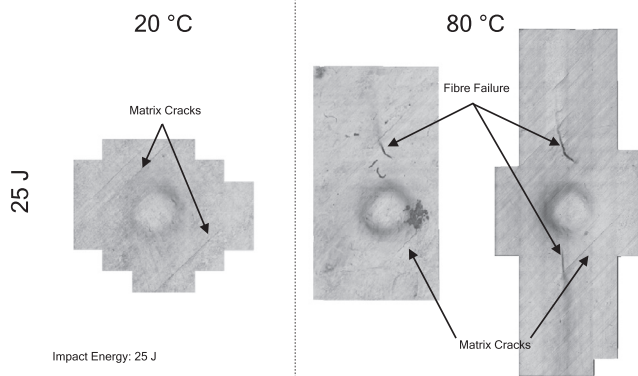


Fig. 9. C-Scan of the delamination damage after impact.

a laser microscope picture of the surface damage of the impact damage from different impact parameters is shown. At 20 °C the area around the impact only exhibits few matrix cracks and a visible permanent indentation. At increased temperature, this changed and fibre damage became visible. The fibres kinked under compression during impact, which results in fibre failure. However, the extent of fibre failure is showing some scatter. Three of five specimens exhibited extensive fibre failure, the difference is shown in Fig. 10.

The residual strength is shown in Fig. 11. The reduction due to the impact damage becomes visible. The residual strength is reduced by 11.1 % when impacted at 20 °C. At impactation at 80 °C the mean residual strength is reduced by 18.58 % compared to the undamaged strength.

In Fig. 12 representative stress-strain curves, obtained by DIC-Measurements of tensile tests are shown displayed. The curve of the of the unimpacted and impacted at 20 °C exhibit linear behaviour until fracture. The sample impacted at 80 °C, which exhibited extensive fibre failure, is showing nonlinear behaviour.

#### 4. Discussion

The presented results exhibit the influence temperature and impact energy on the occurring impact damage. Due to matrix softening, the occurring matrix damage is more localised when temperature is increased. This localisation leads to a more developed permanent indentation depth and fibre failure occurs on the impacted side, as shown by Körbelin et al. [12]. The main part of this study, however, is the influence of this damage on the residual strength.

In Fig. 13 the residual compression strength with additional data from Körbelin et al. [12], which leads to a more comprehensive parameter set, is shown. At an impact energy of 15J and residual strength testing at 20 °C the influence of the delamination size (see Fig. 8) of the

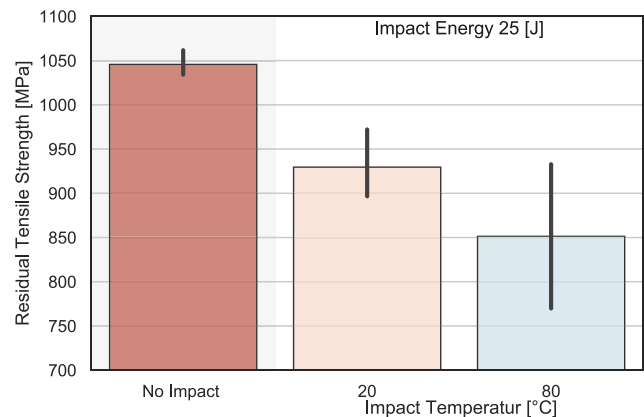


Fig. 11. Tensile strength of unimpacted and impacted tensile specimen at 20 °C and 80 °C.

residual compressive strength is visible. As shown in Fig. 3, the delamination area is increasing at lower temperatures. The larger delamination area leads to earlier material instability and thus lower compressive residual strength. Concluding from this the lowest impact temperature is the most critical - in numerous ways. The indentation depth is the lowest (see Fig. 4) and the indentation depth is showing qualitatively the same behaviour as the residual strength, which means a higher indentation depth is correlating with higher residual strength. Therefore the standard classification of the severity of impact damage with the indentation depth [21] is not leading to a safe evaluation when the temperature is a factor during impactation. Additionally to the limited indentation depth, no fibre failure on the impacted side is visible, making the damage hard to detect visually.

When also taking the residual strength obtained at 80 °C into account, the severe influence of the temperature on the residual compressive strength becomes apparent, see Fig. 13. The residual strength is reduced by a further 10.7 %, when impacted at −20 °C. Whereas the residual strength was spread between 253.8 MPa and 342.6 MPa at 20 °C, at 80 °C the residual strength is only divided between 226.68 MPa and 255.9 MPa. This means that the influence of the different impact damages, and delamination damage in particular, is decreasing because the changing material properties define the stability limit. Therefore the higher ambient temperature is leading to preliminary failure.

When impacted at 21J, the results are not as clear. When only taking the data of different impact temperatures and residual strength testing at 20 °C into account, the impact at −20 °C yields in the lowest residual strength, due to the severely higher delamination area. The lack of

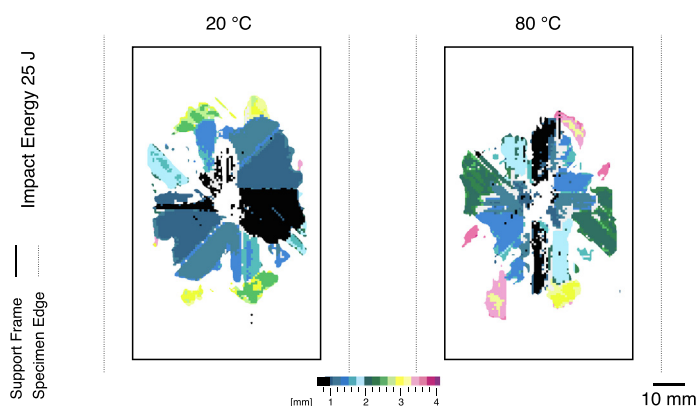
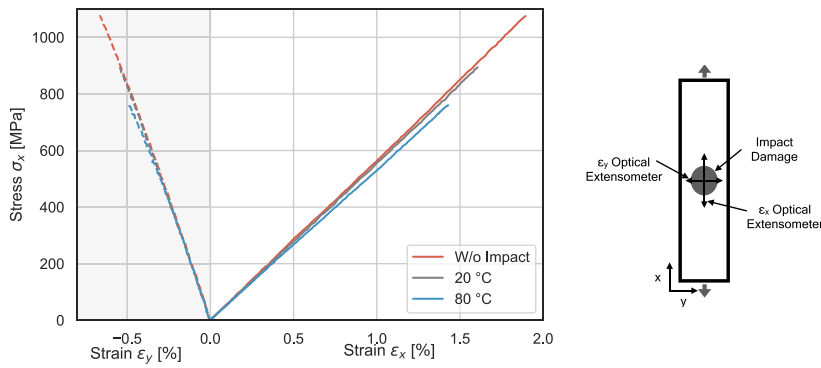
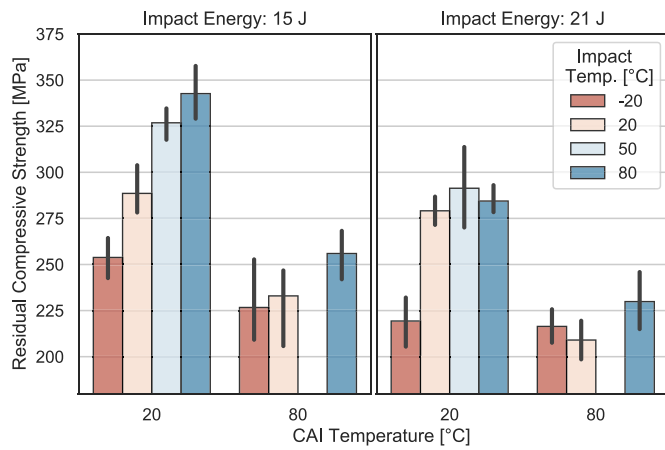


Fig. 10. Impact damage on the impacted side of tensile specimen at 20 °C and 80 °C. The specimens impacted at 80 °C exhibit different severities of fibre failure.



**Fig. 12.** Exemplary tensile stress-strain curves of the tensile tests. Shown are unimpacted and impacted tensile specimen at 20 °C and 80 °C.



**Fig. 13.** Residual compressive strength at different temperatures resulting from different impact temperatures and energies, with additional data from Körbelin et al. [12].

change in residual strength resulting from impacts at 20 to 80 °C could be accounted to the delamination distribution throughout the laminate. As shown in Fig. 5 the delamination distribution at -20 °C is different compared to the other temperatures. The delamination size of impacts at 20 °C and 80 °C does not show significant differences in the delamination distribution in the micrograph, see Fig. 5. One reason for the lack of sensitivity of the residual strength to the projected delamination size could be that in this case, the strength is determined by the test fixture (ASTM 7137 M). Probably larger test specimens and fixture allow to observe the effect of increased projected delamination size on the residual strength.

The retention factor, i.e. the residual strength normalised with the undamaged strength, is an essential parameter for the design of structures. Fig. 14 presents the retention factors, which are normalised to the CAI-Temperature corresponding undamaged strength, e.g. the CAI-Strength determined at 80 °C was normalised to the undamaged strength at 80 °C. Fig. 14 shows that the change in retention factor seems not to be critical, as the values are higher at elevated temperature. The decrease in compressive strength compensates for the nominal differences in residual strength. At both impact energies, the retention factors are higher at 80 °C. However, the scope of residual strengths is closer at 80 °C, which indicates that the influence of the delamination size decreases, which could be due to an improved load diversion based on the lower modulus of the matrix at increased temperature.

However, the investigation of strength under temperature is not common practice. In Fig. 15 the retention factor is shown when only the undamaged compressive strength at 20 °C is used. Here it is shown that especially for 15J the residual strength is not only determined by the

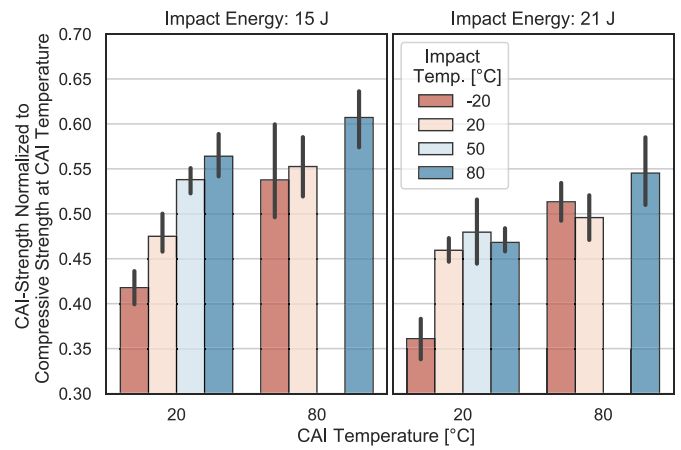


**Fig. 14.** Compressive strength retention after impact normalised to the compressive strength at CAI-Temperature, with additional data from Körbelin et al. [12].

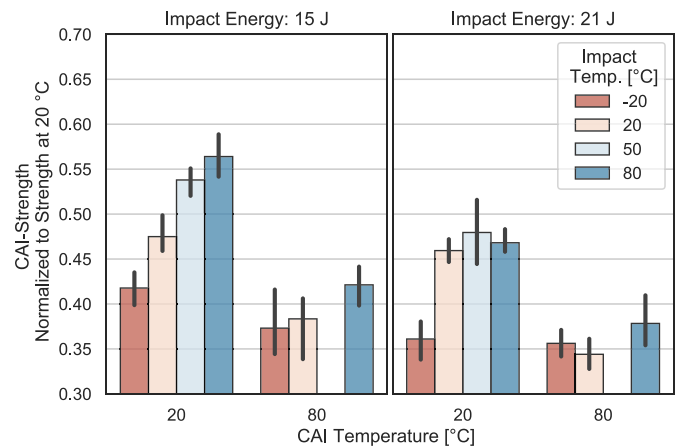


**Fig. 15.** Compressive strength retention after impact normalized to compressive strength at 20 °C. With additional data from Körbelin et al. [12].

impact damage and the impactation parameters but mainly by the temperature at which the residual strength is determined.

The importance of ambient temperature when evaluating the residual strength is particularly evident in Fig. 16, where the resulting cloud of the residual strengths of all tested impactation parameters and residual strengths temperatures, as shown in Fig. 13, is presented. However, the energy is neglected as an influencing factor, only the temperature at which the impact and the residual strength was performed is taken into

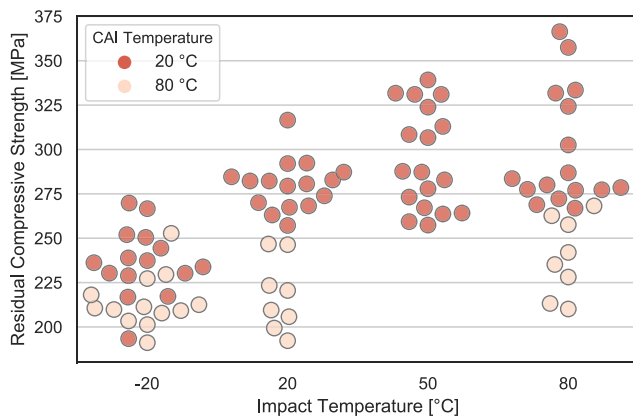


Fig. 16. Residual compressive strength specimens impacted with 15, 18 and 21 J in comparison to impact temperature and CAI-temperature. With additional data from Körbelin et al. [12].

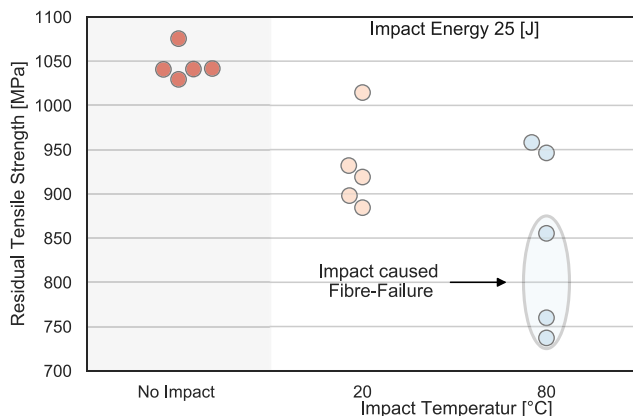


Fig. 17. Tensile and residual tensile strength after impact for different impact temperatures.

account. It becomes clear that the temperature during the compression test has a significant influence on strength.

The tensile results present a different picture. Generally, the decrease in residual strength is not as strong as in compression, but still significant. The results of the tensile tests are shown in more detail in Fig. 17. Here every single tensile-test result is displayed. The strength of the undamaged specimens is exhibiting low scatter. When impacted at 20 °C the scatter increases, which can be explained by the scatter in impact damage, see Fig. 8. The residual strength is reduced due to stress concentrations resulting from the impact damage. At 80 °C the scatter of the residual strength is further increased, ranging from 740 MPa to 950 MPa. This difference in residual strength can be accounted for by the change in fibre failure, see Fig. 10. When just taking the lower three specimens into account, the residual strength drops by 25.01 %. These results confirm that fibre damage reduces the residual strength strongly. Additionally, specimen with fibre failure exhibit a nonlinear stress-strain behaviour, see Fig. 12. This is because the fibre breaks facilitate the transverse contraction. This non-linearity must be taken into account when designing CFRP structures, as it changes the load distribution in the component.

## 5. Conclusion

The present study illustrates that ambient temperature as a variable is crucial to consider composite structures, especially for LVI loaded

structures. With increasing temperature during impactation, the delamination size decreases while the permanent indentation depth and the amount of fibre failure on the impacted side increase. As a result, the detectability of the impact damage increases as well. When considering the residual compressive strength, it is remarkable as the delamination area mainly controls the strength, and thus, the most severe damage is the least detectable. If structures are loaded at elevated temperature, for example, due to solar radiation, the residual compressive strength decrease strongly. As a result, the ambient temperature during compressive loading can have a more significant effect on residual strength than the impact energy. The fibre failure occurring at elevated temperatures on the impacted side has no significant influence on the residual compressive strength, but the tensile properties change, resulting in earlier initiated non-linear behaviour and significantly reduced residual tensile strength. For structures which are mainly loaded in tensile direction, impactation at elevated temperatures is, therefore, a critical load case. For laminates, where the compressive load case is the critical load case, the loading at elevated temperatures is the most critical.

## Acknowledgement

This work was carried out with funding from the German Research Foundation (DFG) within the project number 283641236. This financial support is gratefully acknowledged.

## References

- [1] M. Richardson, M.J. Wisheart, Review of low-velocity impact properties of composite materials, *Compos. Part A: Appl. Sci. Manuf.* 27 (12) (1996) 1123–1131, doi:10.1016/1359-835X(96)00074-7.
- [2] EASA, AMC 20-29: Annex ii - AMC 20-29 to ed decision 2010/003/r (2010).
- [3] Y. Aoki, H. Suemasu, T. Ishikawa, Damage propagation in CFRP laminates subjected to low velocity impact and static indentation, *Adv. Compos. Mater.* 16 (1) (2007) 45–61, doi:10.1163/156855107779755318.
- [4] J. Chang, V. Goyal, J. Klug, Composite structures damage tolerance analysis methodologies. Tech. Rep. nasa/cr-2012-217347, 2012.
- [5] S. Abrate, Impact on laminated composite materials, *Appl. Mech. Rev.* 44 (4) (1991) 155–190, doi:10.1115/1.3119500.
- [6] D. Petersen, R. Rolfes, R. Zimmermann, Thermo-mechanical design aspects for primary composite structures of large transport aircraft, *Aerosp. Sci. Technol.* 5 (2) (2001) 135–146, doi:10.1016/S1270-9638(00)01089-0.
- [7] O. Allix, Modelling and identification of temperature-dependent mechanical behaviour of the elementary ply in carbon/epoxy laminates, *Compos. Sci. Technol.* 56 (7) (1996) 883–888, doi:10.1016/0266-3538(96)00036-X.
- [8] K.D. Cowley, P.W. Beaumont, The interlaminar and intralaminar fracture toughness of carbon-fibre/polymer composites: the effect of temperature, *Compos. Sci. Technol.* 57 (11) (1997) 1433–1444, doi:10.1016/S0266-3538(97)00047-X.
- [9] H.S. Kim, W.X. Wang, Y. Takao, Effects of temperature and stacking sequence on the mode I interlaminar fracture behavior of composite laminates, *Key Eng. Mater.* 183–187 (2000) 815–820, doi:10.4028/www.scientific.net/KEM.183-187.815.
- [10] C. Soutis, D. Turkmen, Moisture and temperature effects of the compressive failure of CFRP unidirectional laminates, *J. Compos. Mater.* (31) (1997).
- [11] Allan Nettles, Hot/wet open hole compression strength of carbon/epoxy laminates for launch vehicle applications (NASA/TM—2009–215900) (2009).
- [12] J. Körbelin, M. Derra, B. Fiedler, Influence of temperature and impact energy on low velocity impact damage severity in CFRP, *Compos. Part A: Appl. Sci. Manuf.* 115 (2018) 76–87, doi:10.1016/j.compositesa.2018.09.010.
- [13] R. Suvarna, V. Arumugam, D.J. Bull, A.R. Chambers, C. Santulli, Effect of temperature on low velocity impact damage and post-impact flexural strength of CFRP assessed using ultrasonic c-scan and micro-focus computed tomography, *Compos. Part B: Eng.* 66 (2014) 58–64, doi:10.1016/j.compositesb.2014.04.028.
- [14] M. Aktas, R. Karakuzu, Y. Arman, Compression-after impact behavior of laminated composite plates subjected to low velocity impact in high temperatures, *Compos. Struct.* 89 (1) (2009) 77–82, doi:10.1016/j.compstruct.2008.07.002.
- [15] G. Short, F. Guild, M. Pavier, The effect of delamination geometry on the compressive failure of composite laminates, *Compos. Sci. Technol.* 2001 (61) (2001) 2075–2086, doi:10.1016/S0266-3538(01)00134-8.
- [16] T. Gómez-del Río, R. Zaera, E. Barbero, C. Navarro, Damage in CFRPs due to low velocity impact at low temperature, *Compos. Part B: Eng.* 36 (1) (2005) 41–50, doi:10.1016/j.compositesb.2004.04.003.
- [17] B. Fiedler, T. Hobbiebrunken, M. Hojo, K. Schulte, Influence of stress state and temperature on the strength of epoxy resins, in: *Proceedings of the 11th International Conference on Fracture 2005, ICF11, 2005*, pp. 2271–2275.
- [18] S. Sánchez-Sáez, E. Barbero, C. Navarro, Compressive residual strength at low temperatures of composite laminates subjected to low-velocity impacts, *Compos. Struct.* 85 (3) (2008) 226–232, doi:10.1016/j.compstruct.2007.10.026.
- [19] W.J. Cantwell, J. Morton, Comparison of the low and high velocity impact response of CFRP, *Composites* 20 (6) (1989) 545–551, doi:10.1016/0010-4361(89)90913-0.

- [20] J. Zhou, B. Liao, Y. Shi, Y. Zuo, H. Tuo, L. Jia, Low-velocity impact behavior and residual tensile strength of CFRP laminates, *Compos. Part B: Eng.* 161 (2019) 300–313, doi:[10.1016/j.compositesb.2018.10.090](https://doi.org/10.1016/j.compositesb.2018.10.090).
- [21] S. Shah, S. Karuppanan, P. Megat-Yusoff, Z. Sajid, Impact resistance and damage tolerance of fiber reinforced composites: a review, *Compos. Struct.* 217 (2019) 100–121, doi:[10.1016/j.compstruct.2019.03.021](https://doi.org/10.1016/j.compstruct.2019.03.021).
- [22] HexPly, M21 datasheet (2018).
- [23] ASTM D7136 / D7136M-15, Test method for measuring the damage resistance of a fiber-reinforced polymer matrix composite to a drop-weight impact event. 10.1520/D7136\_D7136M-15
- [24] ASTM D7137 / D7137M-17, Standard test method for compressive residual strength properties of damaged polymer matrix composite plates(2017). 10.1520/D7137\_D7137M-17
- [25] ASTM D6641 / D6641M-16e1., Test method for compressive properties of polymer matrix composite materials using a combined loading compression (CLC) test fixture. 10.1520/D6641\_D6641M-16E01
- [26] L. Lagunegrand, T. Lorriot, R. Harry, H. Wagnier, J.M. Quenisset, Initiation of free-edge delamination in composite laminates, *Compos. Sci. Technol.* 66 (10) (2006) 1315–1327, doi:[10.1016/j.compscitech.2005.10.010](https://doi.org/10.1016/j.compscitech.2005.10.010).
- [27] M. Gower, R. Shaw, G. Sims, Evaluation of the repeatability under static loading of a compression-after-impact test method proposed for ISO standardisation: DEPC-MN 036, 2005.
- [28] D. McGowan, D. Ambur, Compression response of a sandwich fuselage keel panel with and: Nasa TM 110302, 1997.